Electronic Supplementary Material (ESI) for Environmental Science: Processes & Impacts.
This journal is © The Royal Society of Chemistry 2020

SUPPLEMENTARY MATERIAL

Identifying Patterns and Sources of Anthropogenic Trace Metals in the Argentine Central Andes by using snow samples and an Atmospheric Dispersion Model

S1) EMISSION INVENTORY

An atmospheric emissions inventory (AEI) is one of the three main inputs for the CALPUFF model. These emissions should not only be quantified but also a detailed description of the emitting source and a spatial distribution at an appropriate scale is required.

Currently, there are global, regional or national AEI databases available in different formats that can be implemented in the Air Quality Models. An example of global data collection is the EDGAR database (Emissions Database for Global Atmospheric Research) (European Commission et al., 2016). In its most recent format EDGAR is an AEI in the form of a grid of 0.1° longitude × 0.1° latitude resolution, and it includes pollutants such as greenhouse gases, particulate matter and mercury. Among the regional or continental databases we can mention EMEP (European Environment Agency, 2016) covering Europe. At national level, the US Environmental Agency has organized its national atmospheric emission inventory (NEI) with a disaggregation by geographical division (provincial states, or regions or cities), pollutants (including PM10, CO, NOx, SO2), productive sector (agriculture, energy, industrial processes, etc.), and type of sources (point, area, mobile) (https://www.epa.gov/air-emissions-inventories). Similarly, other countries such as the United Kingdom have their own national databases where they compile relevant information for the estimation of emissions affecting air quality (NAEI: National Atmospheric Emission Inventory, http://naei.defra.gov.uk/overview/). China has developed several emissions inventories, including the Multi-resolution Emission Inventory for China, compiled by Tsinghua University, Beijing (http://www.meicmodel.org/). There are no complete regional inventories for South America, except for those compiled by global databases such as EDGAR. In this sense, there are other inventories for the study area. Puliafito et al. (2015) presented a vehicle activity and emissions inventory with a resolution of 9 km × 9 km for Argentina, where they showed some discrepancies with the EDGAR inventory for the same

study area, especially due to the spatial disaggregation of the base information used. On the other hand, Allende et al. (2016) developed an AEI of persistent organic pollutants for the Great Mendoza area with high spatial resolution (1 km x 1 km).

Considering this information, and that the substances selected in this work are not part of global, regional or previously developed inventories by the authors, an AEI was elaborated as detailed below.

With the aim to ensure accuracy of the estimations calculated, the inventory was performed using two main methodologies, from the data available. A "bottom-up" methodology was used in specific sources, such as industrial sources, disposal and treatment of waste, and mining, in which case there were data of activity levels or whose estimation was possible using the information available. On the other hand, a "top-down" methodology was used for road transport, for which data at a regional level and a lesser level of disaggregation were available.

The anthropic metal emitting sources were identified for the study area from a detailed bibliographic research and are shown in the Table S1. For its categorization, we follow the classification proposed by EMEP/CORINAIR (European Environment Agency, 2016).

Sector	Category	Subcategory	Metal		
			Cu	Pb	Zn
1. Energy	1.A Combustion	1.A.1 Energy industries	x	x	x
		1.A.3.b.i-iv Road transport	x	x	x
	1.B Fugitive emissions from fuels	1.B.2.a.iv Fugitive emissions oil Refining/storage	x	x	x
2. Industrial processes and product use	2.A Mineral products	2.A.1 Cement production	x	x	x
		2.A.3 Glass production		x	
	2.C Metal production	2.C.7.a Copper production	x	x	
		2.C.7.d Storage, handling and transport of metal products (Lead-acid batteries production)		x	
5. Waste	5.C Waste incineration and burning	5.C.1.b.iii Clinical waste incineration	x	x	
		5.C.2 Open burning of waste	x	x	x

Table S1. Source categories for the atmospheric emission inventory.

In all cases, the final calculations were performed using the procedure proposed by EMEP/CORINAIR, according to which an emission factor (F: potential emission of a given substance per reference unit of a product or compound) and a temporal level of activity (A: values of consumption or production) are used to calculate emissions (E) from a known source, according to the equation (1):

$$E = F \times A \qquad (1)$$

The codification of the following subsections corresponds to the categorization proposed by EMEP/CORINAIR.

1. Energy

1.A Combustion

1.A.1 Energy industries

In the study area, there is a power plant complex, with a total of 540 MW installed capacity. The power produced is generated using natural gas, gas oil and fuel as combustibles, resulting in Cu, Pb and Zn emissions.

Combustible	Energy produced [GJ/year] [A]	Emission factor [kg metal/GJ energy produced] [B]		Metal emissions [kg/year] [C]=[A]*[B]	Reference emission factor
Fuel Oil	1.9E06	Cu	5.3E-06	9.9	(European Environment Agency, 2016)
		Pb	4.6E-06	8.5	
		Zn	8.8E-05	163.5	
Gas oil	4.6E05	Cu	2.7E-06	1.2	
		Pb	4.1E-06	1.9	
		Zn	1.8E-06	0.8	
Natural Gas	2.8E07	Cu	7.6E-11	2.2E-03	
		Pb	1.5E-09	4.2E-02	
		Zn	1.5E-09	4.2E-02	
TOTAL			Cu	11.1	
			Pb	10.4	
			Zn	164.3	

Table S2. Calculation of metals emissions resulting from Energy industries

1.A.3.b.i-iv Road transport

Although in many regions metal emissions due to point sources, such as thermal power plants or industrial plants, account for the main contribution to the atmospheric levels, in urban centers road traffic is usually the largest source of these substances. The atmospheric releases occur at ground level mainly due to wear

of brakes, tires, other mechanical components, road pavement, re-suspension of dust and also due to exhaust emissions (Johansson et al. 2009).

For the estimation and distribution in high resolution of the emissions of all road transport, we applied a methodological "top-down" approach detailed in Puliafito et al. (2015). Regarding this, GIS tools associated with the following information were used:

1. Specific data: Maps of localities, annual Average Daily Traffic data (TDMA) and fuel sales by localities.
2. Area or polygons data: population, population density and other economic - social indicators
3. Line data: Street maps and routes classified into accesses, trunk routes, national routes, provincial, primary, secondary and tertiary routes.
4. Satellite data: "Earth at night" satellite images (NOAA-NGDC 2010).

First, the urban areas were redefined using the map of night lights in combination with the population data by district in a grid of 2.5 km resolution. Fuel consumption (gasoline, diesel or CNG) was associated in each district, proportional to the population density of each urban center, distributing it from the convolution between information per grid and a bi-Gaussian filter function. Then the activity (VKT: vehicle transported km) was determined in each cell of the grid, classifying the segments in each cell in hierarchies: accesses, trunks, primary and secondary roads and streets. The daily vehicles in each segment are then determined by dividing the VKT by the length of each segment. This value allows the comparison of these results with the existing TDMA statistics. Finally, the gridded emissions for each pollutant are estimated based on the VKT for each cell and an emission factor for each metal (Sternbeck et al., 2002), adding the contribution of all the segments in each grid.

traveled distance [vehicle.km/year] [A]	Metal emitted	Emission factor [kg metal/vehicle.km] [B]	Metal emission [kg/year] [C] = [A]*[B]	Reference emission factor
5.5E09	Cu	1.7E-07	858.5	(Sternbeck et al., 2002)
	Pb	3.7E-08	184.9	
	Zn	2.4E-07	1197.4	

Table S3. Calculation of metals emissions resulting from road transport

1.B Fugitive emissions from fuels

1.B.2.a.iv Fugitive emissions from oil Refining/storage

In Mendoza, there is an oil refinery located in a Petrochemical Pole south of the urban center, engaged in the manufacture of combustibles and petrochemical substances. The petroleum refinery industry employs

a wide variety of processes, such as separation, conversion, treating, blending, storage and handling. All these processes can emitt metal to the atmosphere (European Environment Agency, 2016).

Crude oil input [t/year] [A]	Metal emitted	Emission factor [kg metal/t cement produced] [B]	Metal emission [kg/year] [C] = [A]*[B]	Reference emission factor
4.4E06	Cu	5.1E-06	22.6	(European Environment Agency, 2016)
	Pb	5.1E-06	22.6	
	Zn	5.1E-06	22.6	

Table S4. Calculation of metals emissions resulting from oil refining/storage

2. Industrial processes and product use

2.A Mineral products

2.A.1 Cement production

Cement production is an unintentional source of metal emissions, due to the kiln's feed material and the nature of the production process. In the study area, there is a cement manufacturing plant located northwest of the urban center of Mendoza, whose kiln uses a mixture that includes hazardous waste and raw material as complement of fuels, in rotary kilns, with dust collector between 200 and 300°C.

Cement production [t/year] [A]	Metal emitted	Emission factor [kg metal/t cement produced] [B]	Metal emission [kg/year] [C] = [A]*[B]	Reference emission factor
736,000	Cu	6.5E-05	47.6	(European Environment Agency, 2016)
	Pb	9.8E-05	72.1	
	Zn	4.2E-04	312.1	

Table S5. Calculation of metal emissions resulting from cement production.

2.A.3 Glass production

In the considered domain, there is a glass manufacturing plant dedicated to the production of bottles, elaborating 6E08 bottles/year, meaning 4.2E05 t/year. The process involves the use of mineral products and a wide range of other materials to achieve properties such as color, clarity and purification, some of which contain lead, resulting in emissions of this metal. The plant operates with continuous furnaces and gases are cleaned with sorbents and electrostatic precipitators or fabric filters.

Glass production [t/year] [A]	Pb Emission factor [kg Pb/t glass produced] [B]	Pb emission [kg/year] [C] = [A]*[B]	Reference emission factor
420,000	2.9E-03	1218	(European Environment Agency, 2016)

Table S6. Calculation of Pb emissions resulting from glass production

2.C Metal production

2.C.7.a Copper production

In the Chilean Andes sector, very close to the border with Argentina, there are two copper mines: "Andina", which produces 2.34E05 t/fine copper per year, and "Los Bronces", which produces 2.0E05 t/fine copper per year. In these mines, in addition to the extraction of minerals from the earth, the conditioning is carried out prior to its transfer to the foundries. Lead anodes are used in one of the process stages, which run out, producing large Pb emissions.

Mine	Copper production [t/year] [A]	metal emitted	kg metal / t copper	Emission [kg/año] [C]=[A]*[B]	Reference emission factor
Andina	2.3E+05	Cu	2.80E-03	6.6E+02	(U.S. Environmental Protection Agency, 1985)
		Pb	1.10E-02	2.6E+03	
Los Bronces	2.0E+05	Cu	2.80E-03	5.6E+02	
		Pb	1.10E-02	2.2E+03	
	TOTAL	Cu		1215	
		Pb		4774	

Table S7. Calculation of metal emissions resulting from copper production

2.C.7.d Storage, handling and transport of metal products (Lead-acid batteries production)

According to data presented by the EPA (U.S. Environmental Protection Agency, 1997) the production of lead-acid batteries is an important source of lead emission worldwide, due to the large amounts of lead compounds used, and the high volumes of manufacture.

In the Greater Mendoza there is a producer of this type of batteries, which produces 42000 batteries / year, from lead oxide which is previously obtained in the same plant.

Batteries produced [batteries/year] [A]	Emission factor Pb [kg Pb/batterie] [B]	Emission Pb [kg/year]	Reference emission factor
42000	7.5E-03	**315.0**	(U.S. Environmental Protection Agency, 1997)

Table S8. Calculation of Pb emissions resulting from lead-acid batteries production

5. Waste

5.C Waste incineration and burning

5.C.1.b.iii Clinical waste incineration

In the study area, the incineration of waste generated in pharmacies, hospitals, health centers and drugstores is performed in a plant located north of the urban centre of Mendoza. Those facilities have a system of pyrolytic thermal destruction of waste where 4.5 t/day of clinical waste are incinerated, making it a source of metals to the atmosphere.

Incinerated medical waste [t/year] [A]	Emitted metal	Emission factor [kg metal/t Incinerated waste] [B]	metal emissions [kg/year] [C]=[A]*[B]	Reference emission factor
1,170	Cu	9.8E-2	114.7	(European Environment Agency, 2016)
	Pb	6.2E-2	72.5	

Table S9. Calculation of metal emissions resulting from clinical waste incineration.

5.C.2 Open burning of waste

Open burning of Municipal Solid Waste (MSW) is probably one of the most significant sources of air pollutants in developing countries (Estrellan and Iino, 2010) and still it is a common practice in the area, where the average generation is 1.18 kg MSW/habitants.day. As stated in the Intergovernmental Panel on Climate Change (IPCC, 2006), in South America, an average of 54% reaches controlled dumping sites, while the rest goes to clandestine waste dumping sites, of which there are no data, and consequently, they have not been considered in this study. Of the waste that reaches these controlled sites, there is a portion made up of paper, cardboard, glass and metal that is separated for reuse by informal workers. Part of the remainder (by 60%) is burnt to reduce its volume and to avoid sources of infection (IPCC, 2006). The burning is performed in the open air without use of appropriate equipment or any control over the emissions. From that information, it was calculated that 350 t MSW/day are burnt.

MSW burned in controlled dumping sites [t/year] [A]	Emitted metal	Emission factor [kg metal/t burned MSW] [B]	metal emission [kg/year] [C]= [A]*[B]	Reference emission factor
129,575	Cu	1.4E-05	1.8	(European Environment Agency, 2016)
	Pb	5.8E-05	7.5	
	Zn	2.5E-05	3.2	

Table S10. Calculation of metal emissions resulting from the open burning of MSW.

SUMMARY OF THE INVENTORY

Sector	Category	Subcategory	Metal		
			Cu	Pb	Zn
1. Energy	1.A Combustion	1.A.1 Energy industries	11.1	10.4	164.3
		1.A.3.b.i-iv Road transport	858.5	184.9	1197.4
	1.B Fugitive emissions from fuels	1.B.2.a.iv Fugitive emissions from oil Refining/storage	22.6	22.6	22.6
2. Industrial processes and product use	2.A Mineral products	2.A.1 Cement production	47.6	72.1	312.1
		2.A.3 Glass production	0	1218	0
	2.C Metal production	2.C.7.a Copper production	1215	4774	0
		2.C.7.d Storage, handling and transport of metal products (Lead-acid batteries production)	0	315	0
5. Waste	5.C Waste incineration and burning	5.C.1.b.iii Clinical waste incineration	114.7	72.5	0
		5.C.2 Open burning of waste	1.8	7.5	3.2
TOTAL			**2271**	**6677**	**1699**

Table S11. Total metal emissions to air in the study area. All emissions are in kg yr^{-1}

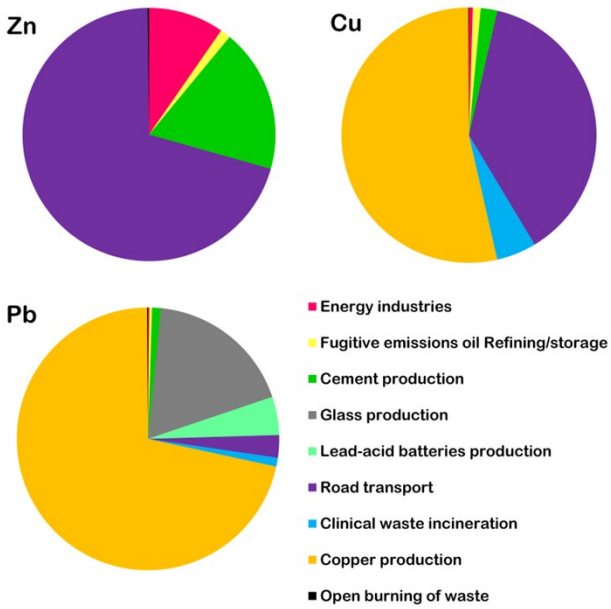

Figure S1. Emissions by source for each metal in the study area

S2) Size distribution of metal emissions

Metals of interest (Cu, Zn and Pb) were modeled as PM of three different aerodynamic diameters: PM10 (10 μm or less); PM2.5 (2.5 μm or less) and PM1 (1 μm or less). For each emitting source, a characteristic size distribution was considered to divide the total emission of each metal estimated in the emission inventory in the PM diameters above-mentioned.

To calculate the size distribution, the percentages presented in Table S12 were multiplied for the total emission previously calculated in the inventory (Table S11).

Metals coming from the source subcategories "Road transport" and "Copper production" are presented in a disaggregated manner, given that they are the result of different emission processes within the same source, as was described in precedent sections.

Source subcategory	Metal	PM1	PM2.5	PM10	Reference
1.A.1 Energy industries	Cu, Pb, Zn	55	23	22	(U.S Environmental Protection Agency, 1995a)
1.A.3.b.i-iv Road transport	Cu	28	48	24	(Pant and Harrison, 2013; U.S. Environmental Protection Agency, 1991)
	Pb	44	39	17	
	Zn	37	33	30	
1.B.2.a.iv Fugitive emissions oil Refining/storage	Cu, Pb, Zn	100	0	0	(U.S Environmental Protection Agency, 1995a
2.A.1 Cement production	Cu, Pb, Zn	10	25	65	(U.S Environmental Protection Agency, 1995b)
2.A.3 Glass production	Pb	20	33	47	(U.S Environmental Protection Agency, 1995c)
2.C.7.a Copper production	Pb	50	30	20	(U.S Environmental Protection Agency, 1995a)
	Cu	10	15	75	(U.S Environmental Protection Agency, 1995d)
2.C.7.d Storage, handling and transport of metal products (Lead-acid batteries production)	Pb	40	25	35	(U.S Environmental Protection Agency, 1995e)
5.C.1.b.iii Clinical waste incineration	Cu, Pb	20	30	50	(U.S Environmental Protection Agency, 1995f)
5.C.2 Open burning of waste	Cu, Pb, Zn	80	14	6	(U.S Environmental Protection Agency, 1995g)

Table S12. Size distribution of particulate metal emissions (%)

S3) Spatial allocation of metal emissions

Source subcategorie	Source type	Location (coordinates in UTM km)		Disaggregation tool
1.A.1 Energy industries	Punctual	X=501.755 km Y= 6342.559 km		Aerial photography + GIS tools
1.A.3.b.i-iv Road transport	Areal	Over the entire road network (Figure 1).		Population density by district+ Road map+Annual Mean Daily Traffic (AMDT)+ DMSP-OLS "Earth at night" satellite data
1.B.2.a.iv Fugitive emissions oil Refining/storage	Areal	(Polygon center) X= 502.447 km Y= 6341.366 km		Aerial photography + GIS tools
2.A.1 Cement production	Punctual	X=514.519 km Y= 6377.648 km		Aerial photography + GIS tools
2.A.3 Glass production	Punctual	X= 523.635 km Y= 6358.008 km		Aerial photography + GIS tools
2.C.7.a Copper production	Areal	(Area center Andina) X= 383.012 km Y= 6331.360 km	(Area center Los Bronces) X= 379.977 km Y= 6331.715 km	Aerial photography + GIS tools
2.C.7.d Storage, handling and transport of metal products (Lead-acid batteries production)	Areal	(Polygon center) X= 517.893 km Y= 6368.742 km		Aerial photography + GIS tools
5.C.1.b.iii Clinical waste incineration	Punctual	X= 518.729 km Y= 6376.870 km		Aerial photography + GIS tools
5.C.2 Open burning of waste	Areal	8 dumping sites distributed in the Mendoza urban area		Aerial photography + GIS tools

Table S13. Total metal emissions to air in the study area. All emissions are in kg/yr.

S4) Implementation of the WRF model

The meteorological data were generated using the coupled regional model Weather Research and Forecasting version 3.5 (Skamarock et al., 2008). It has already been used and validated in the study area (Mulena et al., 2016; S.E. Puliafito et al., 2015). WRF was configured with three nested domains (Figure S2), which comprise the central part of Argentina and Chile, with a spatial resolution of 36, 12 and 4 km respectively; whose vertical coordinate is 50 levels, up to a height of 50 hPa, centered on Latitude 34°4'33.60 "S and Longitude 68°32'38.40" W. The size and location of the domains were selected to

include the Central Andes region with the main hydrographic basins that form part of it and, also, part of the Pacific Ocean to the west to estimate its influence on humidity and regional rainfall (Bolius et al., 2006; Garreaud, 2009). The description of the complex terrain of the area was included by means of digital elevation data from the Shuttle Radar Topography Mission (SRTM3) provided by the USGS Geo Data Center (U.S. Geological Survey, 2017) with an approximate resolution of 90 m that contains a better description of the domain than the default configuration. Likewise, the land use and land cover features by default in WRF were updated with an adaptation of the data map data from European Space Agency (ESA) GLOBCOVER 2009 with a resolution of 300 m, combined with permanent light data from the Operational Linescan System of the DMSP - OLS program for better identification of urban centers, cultivated areas and mountains.

PARAMETRIZATION	CONFIGURATION USED
Terrain features	SRTM3 90 m
land use and land cover features	GLOBCOBER+DMPS-OLS
Initial conditions	Reanalysis NCEP GFS 0.5°
Temporal resolution	90 seconds
Spatial resolution	Three nested domains: 36, 12, 4 (km)
Modeling period	30 days (June 2015)
Vertical resolution	60 levels ETA
Microphysical scheme	ETA microphysics
Long wave radiation	RRTM
Short wave radiation	Goddard Dudhia
Surface	Noah land Surface model
Surface levels	4
Surface physics	Monin-Obukhov similarity Theory
PBL	YSU
EPC	Kain-Fritsch

Table S14. Configurations used in the WRF model for meteorological simulations.

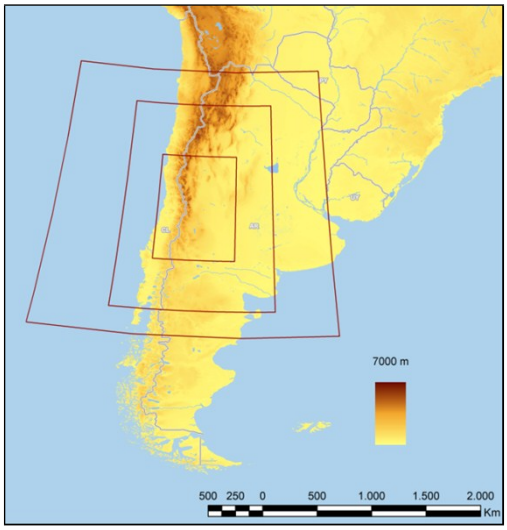

Figure S2. Modeling domains defined for meteorological simulations with WRF

S5) Analytical QA/QC

For quality control of the data, the uncertainties in the measurements were calculated according to the method proposed by Magnusson (2012), and they resulted in 11% for Cu, 25% for Zn and 9% for Pb, all with a 95% confidence, applying a coverage factor k = 2, using reference material ("ICP multi-element standard X CertiPUR® for surface water testing"; traceable to standard reference materials from NIST. Merck, Darmstadt, Germany).

Element	LOD µg L^{-1}	LOQ µg L^{-1}	Reference Material "Standard X"		Recovery of the method (%)
			Measured value µg L^{-1}	Certified value µg L^{-1}	
Cu	0.08	0.17	20.6 +/- 2.27	21 +/- 1	98.3
Zn	0.08	0.45	47.3 +/- 11.8	48 +/- 2	98.6
Pb	0.05	0.17	23.8 +/- 2.14	26 +/- 1	91.6

Table S15. Limits of Detection (LOD) calculated from 3σ and Limits of Quantification (LOQ) calculated from 10σ of 10 replicates of blank solution, and analytical results of reference material "ICP multi-element standard X CertiPUR® for surface water testing".

The analytical blank solution used was a 2% v/v HNO_3 using water of 18 MΩcm and subboiled acid. Based on the analysis of independent blanks, the detection limits of the analytical method were obtained, and they are shown in Table S14.

Trueness of the method was evaluated as the difference between certified and measured values, and it resulted in 5.5% for Cu, 12.5% for Zn and 3.4% for Pb. Precision was evaluated based on the dispersion of the results obtained when measuring the reference material with different analysts, on different days and with the same instrument, and it is 1.7% for Cu, 0.8% for Zn and 2.9% for Pb.

S6) Element concentration values in snow measured by ICP-MS

Tables S15 and S16 show detailed information about the number of samples and the metal concentrations determined for each year in both sampling site.

In a complementary way, the concentrations of other metals, in addition to those studied in this case, were also obtained by ICP-MS, and these results are presented below (Table S17)

VALLECITOS			
	Cu (µg L^{-1})	**Pb (µg L^{-1})**	**Zn (µg L^{-1})**
2014	1.3	2.2	12.8
	1.9	3.7	27.1
2015	1.4	2.4	17.5
	1.5	2	16.7
2016	1.3	1.5	6.6
	1.5	1.5	15
	1.1	1.8	3.7
MAX	1.9	3.7	27.1
MIN	1.1	1.5	3.7
AVERAGE	**1.4**	**2.2**	**14.2**
SD	0.3	0.8	7.7

Table S16. Element concentration values in snow measured by ICP-MS in Vallecitos for every sample, by year.

PUNTA DE VACAS			
	Cu (µg L^{-1})	**Pb (µg L^{-1})**	**Zn (µg L^{-1})**
2014	7.7	3.4	32
	12.9	4.7	58
2015	2.6	2.5	18
	0.8	0.9	4.1
	0.8	0.7	6.2
2016	6.9	3.3	29
	5.3	2.9	21
MAX	12.9	4.7	58
MIN	0.8	0.7	4.1
AVERAGE	5.3	2.6	24.0
SD	4.4	1.4	18.2

Table S17. Element concentration values in snow measured by ICP-MS in Punta de Vacas, for every sample, by year.

	Metal concentration in snow (µg L^{-1}) mean (min-max/SD)	
	Vallecitos	**Punta de Vacas**
Li	0.5 (0.1-1.1/0.6)	1.9 (0.5-4.5/1.7)
Be	<LD	<LD
V	0.9 (<LD-1.0/0.1)	2.4 (0.2-6.2/2.7)
Cr	0.6 (<LD-0.7/0.1)	0.8 (0.6-1.1/0.4)
Mn	18 (12-26/6.6)	87 (8.0 -215/90)
Co	0.3 (0.1-0.6/0.2)	1.3(<LD-2.8/1.2)
Ni	0.3 (<LD-0.5/0.2)	1.4 (0.2-3.9/1.6)
Ti	<LD	<LD
Ga	<LD	<LD
Se	<LD	0.3 (<LD-0.5/0.1)
Sr	2.5 (1.4-4.6/1.3)	12 (3.0-28/11)
Ag	<LD	<LD
Cd	0.2 (<LD-0.2/0.1)	<LD
Cs	<LD	<LD
Ba	4.4 (3.2-8.9/2.5)	18.2 (2.3-41/17.4)
As	<LD	<LD

Table S18. Element concentration values in snow measured by ICP-MS in Vallecitos and Punta de Vacas.

REFERENCES

Allende, D., Ruggeri, M.F., Lana, B., Garro, K., Altamirano, J., Puliafito, E., 2016. Inventory of primary emissions of selected persistent organic pollutants to the atmosphere in the area of Great Mendoza. Emerg. Contam. 2, 14–25. https://doi.org/10.1016/j.emcon.2015.12.001

Bolius, D., Schwikowski, M., Jenk, T., Gäggeler, H.W., Casassa, G., Rivera, A., 2006. A first shallow firn-core record from Glaciar La Ollada, Cerro Mercedario, Central Argentine Andes. Ann. Glaciol. 43, 14–22. https://doi.org/10.3189/172756406781812474

Estrellan, C.R., Iino, F., 2010. Toxic emissions from open burning. Chemosphere 80, 193–207. https://doi.org/10.1016/j.chemosphere.2010.03.057

European Commission, Joint Research Centre (JRC), Netherlands Environmental Assessment Agency (PBL), 2016. Emission Database for Global Atmospheric Research (EDGAR), release version 4.3.1.

European Environment Agency, 2016. EMEP/EEA air pollutant emission inventory guidebook 2016.

Garreaud, R.D., 2009. The Andes climate and weather. Adv. Geosci. 22, 3–11. https://doi.org/10.5194/adgeo-22-3-2009

IPCC, 2006. 2006 IPCC Guidelines for National Greenhouse Gas Inventories. Hayama, Kanagawa JAPAN.

Magnusson, B., Naykki, T., Hovin, H., Krysell, M., 2012. Handbook for Calculation of Measurement Uncertainty in Environmental Laboratories, NT TECHN REPORT 537.

Mulena, G.C., Allende, D.G., Puliafito, S.E., Lakkis, S.G., Cremades, P.G., Ulke, A.G., 2016. Examining the influence of meteorological simulations forced by different initial and boundary conditions in volcanic ash dispersion modelling. Atmos. Res. https://doi.org/http://dx.doi.org/10.1016/j.atmosres.2016.02.009

Pant, P., Harrison, R.M., 2013. Estimation of the contribution of road traffic emissions to particulate matter concentrations from field measurements: A review. Atmos. Environ. 77, 78–97. https://doi.org/10.1016/j.atmosenv.2013.04.028

Puliafito, S.E., Allende, D., Pinto, S., Castesana, P., 2015. High resolution inventory of GHG emissions of the road transport sector in Argentina. Atmos. Environ. 101, 303–311. https://doi.org/10.1016/j.atmosenv.2014.11.040

Puliafito, S.E., Allende, D.G., Mulena, C.G., Cremades, P., Lakkis, S.G., 2015. Evaluation of the WRF Model Configuration for Zonda Wind Events in a Complex Terrain. Atmos. Res. 166, 24–32. https://doi.org/10.1016/j.atmosres.2015.06.011

Skamarock, W.C., Klemp, J.B., Gill, D.O., Barker, D.M., Wang, W., Powers, J.G., 2008. A Description of the Advanced Research WRF Version 3. Mesoscale Microscale Meteorol. Div. Natl. Cent. Atmos. Res.

Sternbeck, J., Sjödin, A., Andreasson, K., 2002. Metal emissions from road traffic and the influence of resuspension. Results from two tunnel studies. Atmos. Environ. 36, 4735–4744. https://doi.org/10.1016/S1352-2310(02)00561-7

U.S. Environmental Protection Agency, 1997. Locating and Estimating Air Emissions from Sources of Lead and Lead Compounds.

Pant, P., Harrison, R.M., 2013. Estimation of the contribution of road traffic emissions to particulate matter concentrations from field measurements: A review. Atmos. Environ. 77, 78–97. https://doi.org/10.1016/j.atmosenv.2013.04.028

U.S Environmental Protection Agency, 1995a. Appendix B.2 Generalized Particle Size Distributions. Compil. Air Pollut. Emiss. Factors, Vol. I Station. Point Area Sources, AP-42 90, 1–22.

U.S Environmental Protection Agency, 1995b. Portland Cement Manufacturing, in: AP-42, Compilation of Air Pollutant Emission Factors.

U.S Environmental Protection Agency, 1995c. Mineral Products Industry: 11.15 Glass Manufacturing, in: Ap 42. pp. 1–10.

U.S Environmental Protection Agency, 1995d. Metallurgical Industry, in: AP-42, Compilation of Air Pollutant Emission Factors Volume I: Stationary Point and Area Sources. pp. 1–20.

U.S Environmental Protection Agency, 1995e. Appendix B.1 Particle size distribution data and sized emission

factors for selected sources, in: AP-42, Compilation of Air Pollutant Emission Factors. pp. 1–103.

U.S Environmental Protection Agency, 1995f. Medical Waste Incineration, in: AP-42, Compilation of Air Pollutant Emission Factors.

U.S Environmental Protection Agency, 1995g. Refuse Combustion, in: AP-42, Compilation of Air Pollutant Emission Factors.

U.S. Environmental Protection Agency, 1991. Compilation of air pollutant emission factors. Volume II: Mobile Sources.

U.S. Environmental Protection Agency, 1985. Sources of copper air emmissions.

U.S. Geological Survey, 2017. Earth Explorer [WWW Document]. URL https://earthexplorer.usgs.gov/